

Laboratori Nazionali di Frascati

LNF-92/022 (P)

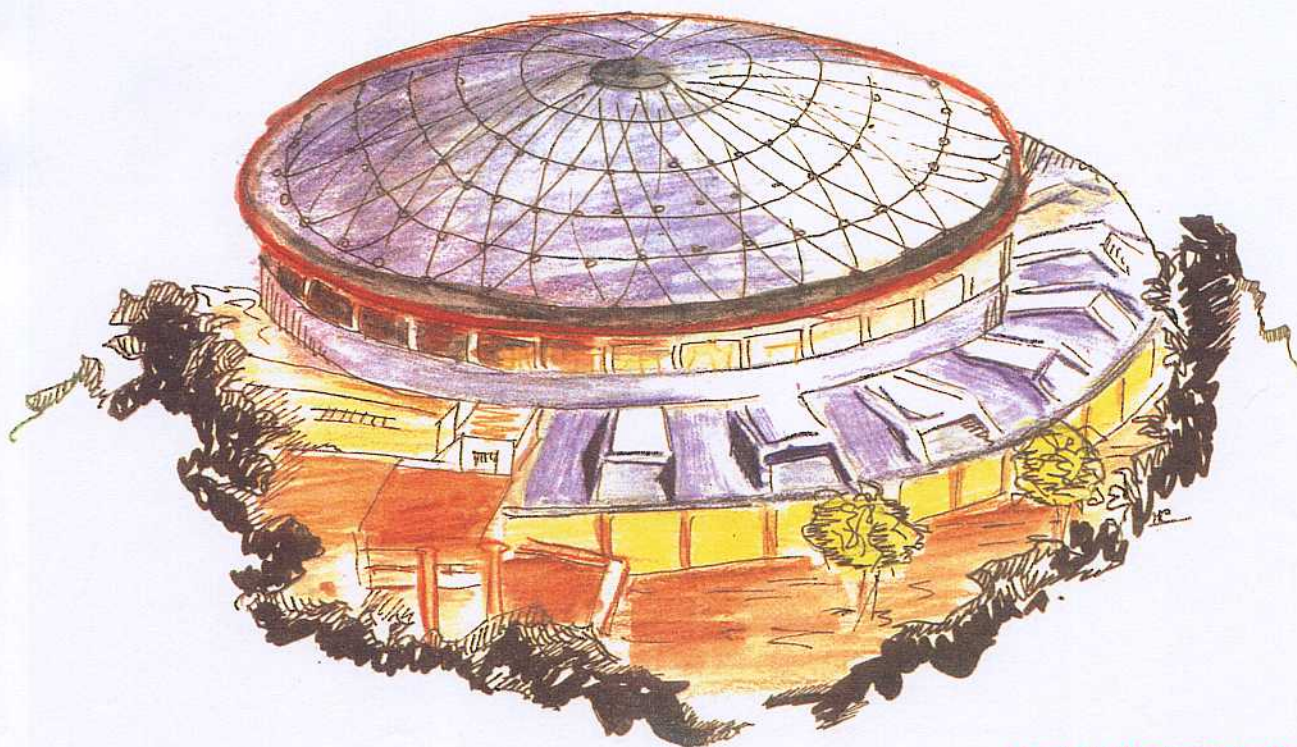
8 Aprile 1992

ENSLAPP-A-373/92

A. Bramon, G. Colangelo, P.J. Franzini, M. Greco

$\phi \rightarrow \pi^+ \pi^- \gamma$ AT DAΦNE

Contribution to the DAΦNE Physics Handbook



Servizio Documentazione
dei Laboratori Nazionali di Frascati
P.O. Box, 13 - 00044 Frascati (Italy)

LNF-92/022 (P)
8 Aprile 1992

ENSLAPP-A-373/92

$\phi \rightarrow \pi^+ \pi^- \gamma$ at DAΦNE

A. Bramon

Grup de Física Teòrica, Universitat Autònoma de Barcelona,
08193 Bellaterra (Barcelona), Spain

G. Colangelo

INFN, Laboratori Nazionali di Frascati,
P.O.Box 13, 00044 Frascati, Italy

P.J. Franzini

Laboratoire de Physique Théorique ENSLAPP,
BP110, F74941, Annecy-le-vieux, Cedex, France

M. Greco

Dipartimento di Fisica Nucleare e Teorica dell'Università, I-27100, Pavia, Italy
and INFN, Laboratori Nazionali di Frascati, I-00044, Frascati, Italy

Abstract

The possible detection of the reaction $\phi \rightarrow f_0(975)\gamma \rightarrow \pi^+\pi^-\gamma$ at DaΦne is discussed together with the initial and final state background radiation. The size of the effect is shown to depend crucially on the relative sign of the $e^+e^- \rightarrow \rho \rightarrow \pi^+\pi^-\gamma$ and $e^+e^- \rightarrow \phi \rightarrow f_0\gamma \rightarrow \pi^+\pi^-\gamma$ amplitudes. A detailed study of the angular distributions as well as numerical results are also given.

Projected high-luminosity, low-energy e^+e^- machines, such as the DaΦne Φ-Factory, will allow for the detection and measurement of rare decay modes of the well-known, low-lying vector mesons. The $\phi \rightarrow \pi^+\pi^-\gamma$ decay, whose branching ratio is known to be smaller than $7 \cdot 10^{-3}$ [1], will probably be studied in the near future due to the (relatively) clean signature of a charged pion pair with a photon of energy larger than some 20 MeV. In this case, not only the properties of the ϕ -meson will be explored but also those of the final pion-pair and, in particular, their resonant states such as the controversial f_0 -scalar meson at 975 MeV [2]. The purpose of this paper is to discuss the possible detection of such an f_0 -signal under a considerably large background. The main two sources for the latter are expected to be initial-state bremsstrahlung and ρ -formation followed by its (off-shell) decay into $\pi^+\pi^-\gamma$. In the first case, the pion pair is in a negative charge-conjugation state, while the opposite is true for the second as well as for the pion pair in any genuine $\phi \rightarrow \pi^+\pi^-\gamma$ radiative decay. Interference effects will be important between these two latter (C=+) amplitudes, but those with the first one (C=-) will disappear when integrating over pion angles disregarding their charges [3].

The most obvious and important background comes from initial-state hard photon radiation. One obtains [4]

$$d\sigma/dE|_{in} = 2\sigma_0(s(1-x))H(x, s, \theta_{min})/\sqrt{s} \quad (1)$$

where σ_0 stands for the non-radiative $e^+e^- \rightarrow \rho \rightarrow \pi^+\pi^-$ cross-section

$$\sigma_0(s) = \frac{\pi \alpha^2}{3 s} |F_\rho(s)|^2 (1-\xi)^{3/2}, \quad (2)$$

x is related to the photon energy E through $x \equiv 2E/\sqrt{s}$, $\xi \equiv 4m_\pi^2/s$, and

$$H(x, s, \theta_{min}) = \frac{\alpha}{\pi} \frac{2(1-x) + x^2}{x} \left[\ln \left(\frac{1 + \beta \cos \theta_{min}}{1 - \beta \cos \theta_{min}} \right) - \frac{1}{\gamma^2} \frac{\cos \theta_{min}}{1 - \beta^2 \cos^2 \theta_{min}} \right]. \quad (3)$$

In eq. (3), θ_{min} is the minimal angle (with respect to the beam direction) allowed for the photon to be detected. The radiator $H(x, s, \theta_{min})$ is obtained from the angular distribution ¹ $d\sigma/d\cos\theta_\gamma \simeq \sin^2\theta_\gamma/(1 - \beta^2\cos^2\theta_\gamma)^2$ and reduces to the well known integrated radiator

$$H(x, s) = \frac{\alpha}{\pi} \left[\frac{2(1-x) + x^2}{x} \left(\ln \frac{s}{m_e^2} - 1 \right) \right], \quad (4)$$

for $\theta_{min} = 0$. Finally $F_\rho(s)$ in eq. (2) stands for the ρ -dominated pion form-factor [5]

$$F_\rho(s) = \frac{M_\rho^2}{M_\rho^2 - s - i\sqrt{s}\Gamma_\rho}. \quad (5)$$

¹See the appendix for the complete expression

The resulting differential cross-section for initial-state radiation is shown in Fig.1 for $\theta_{\min} = 0$ (solid line) and for $\theta_{\min} = 10^\circ$ (dotdashed line).

The second source of background comes from off-shell ρ -formation followed by radiative decay into a $C=+$ pion pair. The corresponding, gauge- invariant amplitude is given by

$$A(\rho \rightarrow \pi^+ \pi^- \gamma) = 2\sqrt{2}eg \left[\frac{\epsilon p_+}{qp_+} \epsilon^* \left(p_- - \frac{1}{2}q^* \right) + \frac{\epsilon p_-}{qp_-} \epsilon^* \left(p_+ - \frac{1}{2}q^* \right) + \epsilon \epsilon^* \right] \quad (6)$$

where $g=4.2$ comes from the total ρ width of 149 MeV, p_+ , p_- and q are the pion and photon four-momenta, and ϵ, ϵ^* are the polarizations of the photon and the ρ . The correctness of this amplitude can easily be tested by comparing with the measured decay rate of on-shell ρ mesons into a pion pair and a photon of energy E larger than 50 MeV. One immediately obtains a partial width of 1.62 MeV in good agreement with the observed value of 1.48 ± 0.24 MeV ([1, 6], see also [7]). The effect of the above amplitude around the ϕ -peak requires the introduction of the ρ dominated form factor $F_\rho(s)$. One easily obtains the following differential cross-section

$$d\sigma/dE|_\rho = 2\sigma_0(s) F(x, s)/\sqrt{s} \quad (7)$$

with

$$F(x, s) = \frac{\alpha}{\pi} \frac{2}{(1-\xi)^{3/2}} \left[\left(x - (1-\xi) \frac{1-x}{x} \right) \sqrt{1 - \frac{\xi}{1-x}} \right. \\ \left. + (1-\xi)(1-x - \xi/2) \frac{1}{x} \ln \left| \frac{1 + \sqrt{1 - \frac{\xi}{1-x}}}{1 - \sqrt{1 - \frac{\xi}{1-x}}} \right| \right] \quad (8)$$

where small corrections coming from higher order terms in x have been neglected. For s on the ϕ -peak, the values of the above expression are shown (dashed line) in Fig.1. Typically, they are one order of magnitude below the previously considered background coming from the initial-state radiation with $\theta_{\min} = 0$.

We now turn to the ϕ signal as produced through the $\phi \rightarrow f_0 \gamma \rightarrow \pi^+ \pi^- \gamma$ decay chain. Amplitudes and couplings for each step are defined according to

$$A(\phi \rightarrow f_0 \gamma) = eG_s [(\epsilon^* \epsilon) (q^* q) - (\epsilon^* q) (\epsilon q^*)] \equiv eG_s \{a\}, \quad (9)$$

$$A(f_0 \rightarrow \pi^+ \pi^-) = g_s.$$

where now ϵ^* and q^* stand for the ϕ polarization and four-momentum. These amplitudes lead to the following decay rates

$$\Gamma(\phi \rightarrow f_0 \gamma) = \frac{1}{12\pi} G_s^2 e^2 |\vec{q}_\gamma|^3 \quad (10)$$

$$\Gamma(f_0 \rightarrow \pi^+ \pi^-) = \frac{2}{3} \Gamma(f_0 \rightarrow \pi \pi) = \frac{1}{8\pi} g_s^2 \frac{|\vec{p}_+|}{m_f^2}$$

From these expressions and the experimental values quoted in [1] one obtains the modulus of the product of the relevant coupling constants in terms of the unknown branching ratio $\text{BR}(\phi \rightarrow f_0 \gamma)$

$$|G_s g_s| = (144 \pm 15)(BR(\phi \rightarrow f_0 \gamma))^{1/2} \quad (11)$$

The amplitude for the ϕ decay into $f_0 \gamma \rightarrow \pi^+ \pi^- \gamma$ then follows

$$A(\phi \rightarrow \pi^+ \pi^- \gamma) = e g_s G_s P_f(s') \{a\} \quad (12)$$

with

$$P_f(s') = \frac{1}{m_f^2 - s' - i m_f \Gamma_f} \quad (13)$$

$\{a\}$ as in eq.(9), $s' = s(1-x)$ and $s = q^*{}^2 = M_\phi^2$ on the ϕ -peak.

As previously stated, the off-shell ρ -amplitude in an e^+e^- experiment interferes with the just derived (near on-shell) one for the ϕ . The total amplitude (with $C=+$) may be written as

$$A^+(\gamma^* \rightarrow \pi^+ \pi^- \gamma) = \frac{e}{f_\rho} F_\rho(s) A(\rho \rightarrow \pi^+ \pi^- \gamma) + \frac{e}{f_\phi} F_\phi(s) A(\phi \rightarrow \pi^+ \pi^- \gamma) \quad (14)$$

where $f_\phi = -3f_\rho/\sqrt{2} = -3g$, $F_{\rho,\phi}(s)$ are form factors and $A(\rho, \phi \rightarrow \pi^+ \pi^- \gamma)$ are given in eqs.(6) and (12).

Integrating over the pion energies the C-even amplitude (14) leads to the differential cross-section

$$d\sigma/dE|_{\rho+\phi} = d\sigma/dE|_\rho + d\sigma/dE|_\phi + d\sigma/dE|_{int} \quad (15)$$

where the ρ -term has been given in eq.(7), and the ϕ - and interference-terms (the ϕ -signal) are given by

$$d\sigma/dE|_\phi = \frac{2\alpha^3}{3s} \left(\frac{g_s G_s}{3g} \right)^2 |F_\phi(s) P_f(s(1-x))|^2 E^3 \sqrt{1 - \frac{\xi}{1-x}} \quad (16)$$

$$d\sigma/dE|_{int} = \frac{-4\alpha^3}{3s} \frac{g_s G_s}{3g} \text{Re} \left(F_\rho^*(s) F_\phi(s) P_f(s') \right) \quad (17)$$

$$E \left(\sqrt{1 - \frac{\xi}{1-x}} + \frac{\xi}{2} \ln \left| \frac{1 - \sqrt{1 - \frac{\xi}{1-x}}}{1 + \sqrt{1 - \frac{\xi}{1-x}}} \right| \right)$$

The corresponding expressions before integration over the angle θ_γ and pion energies, can be found in the Appendix, where we also present some detailed studies of the angular distributions. Eqs.(16) and (17) contain the unknown product $g_s G_s$, i.e., relevant information on the f_0 -meson and, more specifically, on the $BR(\phi \rightarrow f_0 \gamma)$ as indicated in eq.(11). Theoretical estimates of this branching ratio range from 10^{-3} to 10^{-6} . Recent analyses by Brown and Close [2] indicate $BR(\phi \rightarrow f_0 \gamma) = 1.36 \cdot 10^{-4}$ (if a calculation along the lines of [8] is performed), 10^{-4} (if the f_0 is a $q\bar{q}q\bar{q}$ system) or 10^{-5} (if the f_0 were pure $s\bar{s}$). Since the last possibility is not entirely reasonable for an f_0 -meson decaying mainly in two pions, smaller values for the branching ratio should also be considered. For all these reasons we present our results in Figs.2 and 3 for three values of $BR(\phi \rightarrow f_0 \gamma)$ in eq.(11), namely, 10^{-4} (solid lines), 10^{-5} (dashed lines) and 10^{-6} (dotted lines). Fig.2 shows the photonic spectra coming from

the terms quoted in eq.(16) (positive curves) and eq.(17) (negative curves). This corresponds to choosing the positive sign for $g_s G_s$ in eq.(11). In this case the effects of the ϕ -decay tend to cancel when interfering with the off-shell $\rho \rightarrow \pi^+ \pi^- \gamma$ - decay. Fig.3a, where the values for $1 + d\sigma(\text{signal})/d\sigma(\text{background})$ have been plotted, shows the remaining effects of the order of a few percent. Choosing the negative sign for $g_s G_s$, reverses the sign of the interference term shown in the lower half of Fig.2, thus enhancing the effect. This is clearly seen in Fig.3b where now the ratio between the signal and the background can reach a 50%. In all these curves we have assumed $\theta_{\min} = 10^\circ$, which seems reasonable for a ϕ -factory [9]. If we had integrated over the whole radial angle, the signal over background ratio would have reduced by a factor of 2.5.

In summary, the possibilities of detecting and analysing the decay chain $\phi \rightarrow f_0 \gamma \rightarrow \pi^+ \pi^- \gamma$ depend rather crucially on the relative sign between this amplitude and the one describing off-shell $\rho \rightarrow \pi^+ \pi^- \gamma$ decay. The latter is only a minor part of the whole background dominated by non-interfering radiation from the $e^+ e^-$ initial state. In spite of this, a rather clean effect is predicted if the ϕ - and ρ -amplitudes are on-phase, while the effect tends to disappear in the opposite case, which is a priori equally probable.

Appendix - Angular distributions.

Here we give the expressions of the differential cross sections obtained squaring the amplitude given in eq.(14), before making any integration. We must first define the relevant angles (see Fig. 4): we choose the photon momentum along the z axis and the projection of the beam in the plane perpendicular to the photon to be the y axis. The direction of one pion is then given by its polar and azimuthal angles in this system: θ , the angle between this pion and the photon, and ϕ_π , the angle between the projections of the pion direction and beam direction onto the xy plane, or, equivalently, between the $e^+e^-\gamma$ plane and the $\pi^+\pi^-\gamma$ plane. The direction of the beam is specified by the photon-beam angle θ_γ , and an azimuthal angle of zero. The direction of the second pion is completely specified by kinematics; in addition we have a relation between θ and the photon and pion energies:

$$\cos \theta = \frac{1}{\beta} \left[\frac{2(1-x-y)}{xy} + 1 \right] \equiv \frac{A}{x\sqrt{B}}; \quad \beta = \sqrt{1 - \xi/y^2} \equiv \sqrt{B}/y \quad (18)$$

where we have introduced the abbreviations $x = 2E_\gamma/\sqrt{s}$, $y = 2E_+/\sqrt{s}$, E_+ is the energy of the π^+ , $\xi = 4m_\pi^2/s$, $A = 2(1-x-y) + xy$, and $B = y^2 - \xi$. We will also find it convenient to define the angle between the pion and the beam, θ_π , which is related to the previously defined quantities by

$$\cos \theta_\pi = \cos \theta \cos \theta_\gamma + \cos \phi_\pi \sin \theta \sin \theta_\gamma. \quad (19)$$

Finally, we also define the physically more useful angle $\theta_{\pi\gamma}$, the angle between the pions and the photon *in the dipion rest frame* by the relation

$$y = 1 - \frac{x}{2} \left(1 + \cos \theta_{\pi\gamma} \sqrt{1 - \frac{\xi}{1-x}} \right). \quad (20)$$

We have then the following expression for $d^3\sigma$: for $\phi \rightarrow f_0\gamma$,

$$\frac{d^3\sigma^\phi}{dE_\gamma d\cos\theta_\gamma dE_+} = \frac{\alpha^3}{4s} \left(\frac{g_s G_s}{3g} \right)^2 |F_\phi(s) P_f(s(1-x))|^2 E^2 \sqrt{1 - \frac{\xi}{1-x}} (1 + \cos^2\theta_\gamma) \quad (21)$$

where the subsequent f_0 decay to two pions is modelled with a standard s wave distribution. For the process $\rho \rightarrow \pi\pi\gamma$, we have

$$\frac{d^4\sigma^\rho}{dE_\gamma d\cos\theta_\gamma dE_+ d\phi_\pi} = \frac{2\alpha^3}{s} |F_\rho(s)|^2 \frac{1}{2\pi} T_1 \quad (22)$$

with

$$\begin{aligned}
T_1 = & 4 + \frac{\xi/2}{(1-x-y)^2} \left[4(x+y+\xi/4-1) \right. \\
& \left. - x^2(1-\cos^2\theta_\gamma) - y^2(1-\beta^2\cos^2\theta_\pi) - 2xy(1-\beta\cos\theta_\pi\cos\theta_\gamma) \right] \\
& + \frac{\xi}{4(1-y)^2} \left[2\xi - 2y^2(1-\beta^2\cos^2\theta_\pi) \right] \\
& + \frac{2-\xi}{(1-y)(x+y-1)} \left[2(1-x-y-\xi/2) \right. \\
& \left. + y^2(1-\beta^2\cos^2\theta_\pi) + xy(1-\beta\cos\theta_\pi\cos\theta_\gamma) \right]
\end{aligned} \tag{23}$$

For the interference term we have

$$\frac{d^4\sigma^{int}}{dE_\gamma d\cos\theta_\gamma dE_+ d\phi_\pi} = \frac{\alpha^3}{4s} \frac{g_s G_s}{3g} \operatorname{Re} \left(F_\rho^*(s) F_\phi(s) P_f(s') \right) \frac{1}{2\pi} T_2 \tag{24}$$

with

$$\begin{aligned}
T_2 = & 4x + \frac{2-x-y}{1-y} \left[xy(1-\beta\cos\theta_\pi\cos\theta_\gamma) - 2(x+y-1) \right] \\
& - \frac{y}{1-x-y} \left[2(x+y-1) - x^2(1-\cos^2\theta_\gamma) - xy(1-\beta\cos\theta_\pi\cos\theta_\gamma) \right] \\
& + \frac{x^2}{(1-y)(x+y-1)} \left[2(1-x-y-\xi/2) \right. \\
& \left. + xy(1-\beta\cos\theta_\pi\cos\theta_\gamma) + y^2(1-\beta^2\cos^2\theta_\pi) \right]
\end{aligned} \tag{25}$$

Using eqs. (18) and (19) for θ and θ_π and integrating over ϕ_π , we have

$$\begin{aligned}
\int T_1 \frac{d\phi_\pi}{2\pi} = & 4 \\
& - \frac{\xi}{(1-x-y)^2} \left[\left(A + \frac{x^2}{2} \right) (1-\cos^2\theta_\gamma) + \frac{B}{4} (1+\cos^2\theta_\gamma) + \frac{A^2}{4x^2} (1-3\cos^2\theta_\gamma) \right] \\
& - \frac{\xi}{4(1-y)^2} \left[B(1+\cos^2\theta_\gamma) + \frac{A^2}{x^2} (1-3\cos^2\theta_\gamma) \right] \\
& + \frac{2-\xi}{(1-y)(x+y-1)} \left[A(1-\cos^2\theta_\gamma) + \frac{B}{2} (1+\cos^2\theta_\gamma) + \frac{A^2}{2x^2} (1-3\cos^2\theta_\gamma) \right]
\end{aligned} \tag{26}$$

$$\begin{aligned}
& \int T_2 \frac{d\phi_\pi}{2\pi} = 4x \\
& + \frac{2-x-y}{1-y} A (1 - \cos^2 \theta_\gamma) \\
& + \frac{y}{1-x-y} (A + x^2) (1 - \cos^2 \theta_\gamma) \\
& + \frac{x^2}{(1-y)(x+y-1)} \left[A (1 - \cos^2 \theta_\gamma) + \frac{B}{2} (1 + \cos^2 \theta_\gamma) + \frac{A^2}{2x^2} (1 - 3\cos^2 \theta_\gamma) \right]
\end{aligned} \tag{27}$$

It may be easily checked that integrating eqs. (21), (26) and (27) over $d \cos \theta_\gamma$ and dE_+ , in the limit $x \ll 1$, one recovers eqs. (8), (16) and (17).

For the initial state radiation, the distribution has already been given (see for example [3], [4]). For convenience, we reproduce the result here:

$$\begin{aligned}
\frac{d^4\sigma}{d\Phi} &= \frac{2e^2 |F_\pi(t)|^2 \beta_\pi^2 \sin^2 \theta_\gamma}{t(s-t)^2 (1 - \beta_e^2 \cos^2 \theta_\gamma)^2} \\
& \left[(s+t)^2 (1 + \cos^2 \theta_\gamma) - [2\sqrt{st} \sin \theta_\gamma \sin \theta_{\pi\gamma} \cos \phi + (s+t) \cos \theta_\pi \cos \theta_{\pi\gamma}]^2 \right]
\end{aligned} \tag{28}$$

with the phase space factor

$$d\Phi = \frac{\beta_\pi E_\gamma}{2(4\pi)^4 M_\phi^2} dE_\gamma d \cos \theta_\gamma d \cos \theta_{\pi\gamma} d\phi_\pi. \tag{29}$$

Here β_e is the velocity of the electron in the lab frame, and β_π the velocity of the pions in the dipion rest frame, given by

$$\beta_\pi = \sqrt{1 - \xi/(1-x)}. \tag{30}$$

Our distributions are shown in Figs. 5-8.

Acknowledgements We would like to thank J. Lee-Franzini and Paolo Franzini for emphasizing the importance of a careful study of the angular distributions, and particularly W. Kim for producing the elaborate three-dimensional plots illustrating this note.

References

- [1] PDG. Phys. Lett. B 239 (1990)
- [2] N.Brown and F.E.Close, this report.
N.N. Achasov and V.N. Ivanchenko, Nucl. Phys. B315 (1989) 476.
- [3] M.J. Creutz and M.B.Einhorn, Phys. Rev. D1 (1970) 2537
P. Singer, Phys. Rev. 130 (1963) 2421 and (E) 161 (1967) 1694.
- [4] M.Greco Riv. Nuovo Cim. 11 (1988) 1,
G.Bonneau and F.Martin, Nucl. Phys. B27 (1971) 381.
- [5] The use of a more sophisticated version of the pion form factor, as in G.Colangelo, S.Dubnicka and M.Greco, this Report, in the ϕ -region, introduces numerically irrelevant effects.
- [6] S.I.Dolinsky et al. Phys. Rep. C202 (1991) 99
I.B.Vasserman et al., Sov. J. Nucl. Phys. 47 (1988) 1035.
- [7] S: Fajfer and R.J. Oakes, Phys. Rev. D44 (1991) 1599,
notice that the $\rho \rightarrow \pi^+\pi^-\gamma$ amplitude in this work apparently is not gauge invariant.
- [8] J.L.Lucio and J.Pestieau Phys.Rev. D 42 (1990) 3253,
S.Nussinov and T.N. Truong Phys.Rev.Lett. 63 (1989) 2003.
- [9] J.Lee-Franzini, W.Kim and P.J.Franzini, this report.

FIGURE CAPTIONS

- Fig. 1** Differential cross-sections as a function of the photon energy E for initial state, hard photon radiation, $e^+e^- \rightarrow \rho^0\gamma \rightarrow \pi^+\pi^-\gamma$ (solid line for $\theta_{min} = 0$ and dotdashed line for $\theta_{min} = 10^\circ$) and for off-shell ρ -formation and decay $e^+e^- \rightarrow \rho \rightarrow \pi^+\pi^-\gamma$ (dashed line).
- Fig. 2** Contributions to the differential cross-section for $e^+e^- \rightarrow \pi^+\pi^-\gamma$ on the ϕ -peak as a function of the photon energy E coming from the ϕ -terms in eq.(16) (upper curves) and the interference term in eq.(17) (lower curves). G_s, g_s is taken from the positive root in eq.(10) for $BR(\phi \rightarrow f_0\gamma) = 10^{-4}, 10^{-5}$ and 10^{-6} (solid, dashed and dotted lines, respectively). $\theta_{min} = 10^\circ$.
- Fig. 3** Ratio between the $\phi \rightarrow f_0\gamma \rightarrow \pi^+\pi^-\gamma$ signal and the background as a function of the photon energy E . Solid, dashed and dotted curves correspond to $BR(\phi \rightarrow f_0\gamma) = 10^{-4}, 10^{-5}$ and 10^{-6} in eq.(10) with a) the positive root (destructive interference) and b) the negative (constructive) one. $\theta_{min} = 10^\circ$
- Fig. 4** Definition of the angles used in this paper.
- Fig. 5-8 a,b** Shapes of the angular distribution; two views: a, $d\sigma/dE_\gamma d\cos\theta_\gamma$, and b, $d\sigma/dE_\gamma d\cos\theta_{\pi\gamma}$ (equivalent to $d\sigma/dE_\gamma dE_\pi$), for the various terms contributing to the cross section: 5, initial state radiation; 6, off shell ρ production; 7, interference of off-shell ρ and f_0 production; 8, f_0 production. In figs. 7 and 8 we have used $BR(\phi \rightarrow f_0\gamma) = 2.5 \cdot 10^{-4}$; in fig. 7 we have used the negative root of eq. (11), that is the case of constructive interference. The angle $\theta_{\pi\gamma}$ used here is the angle between the pions and the photon *in the dipion rest frame* (see text).

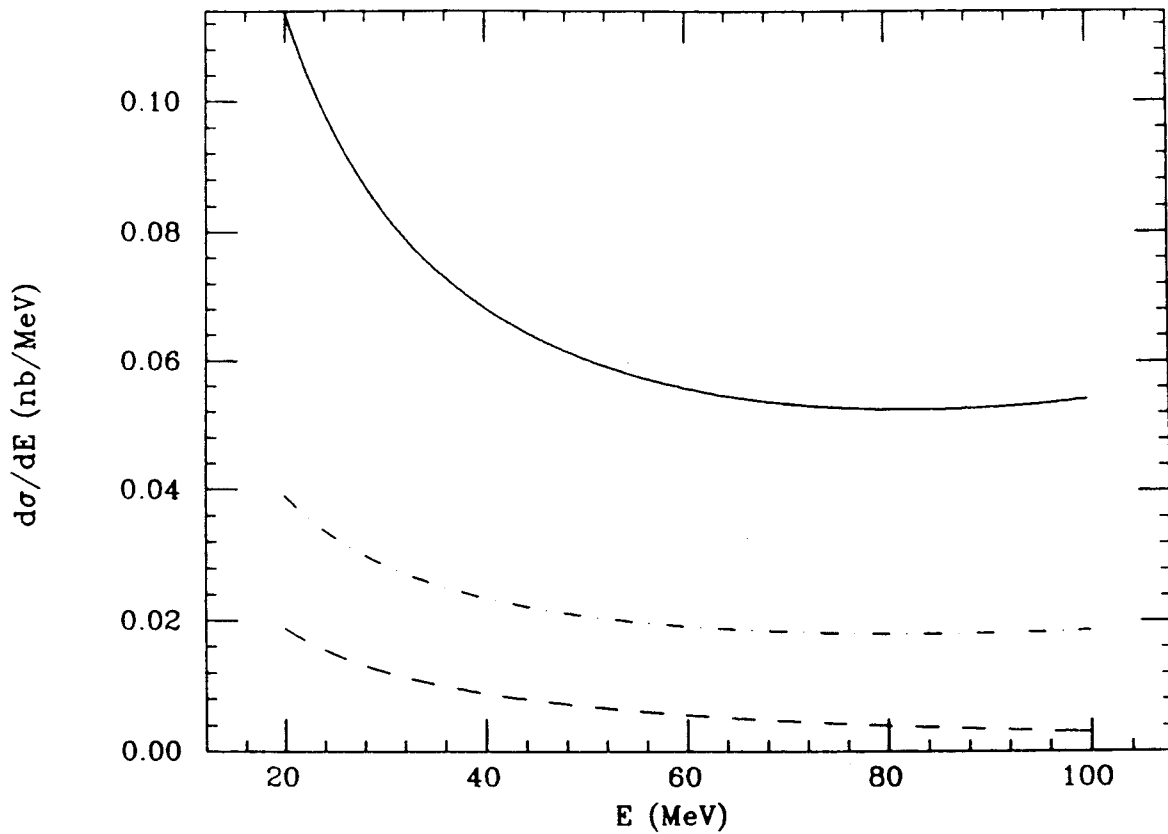


FIG. 1

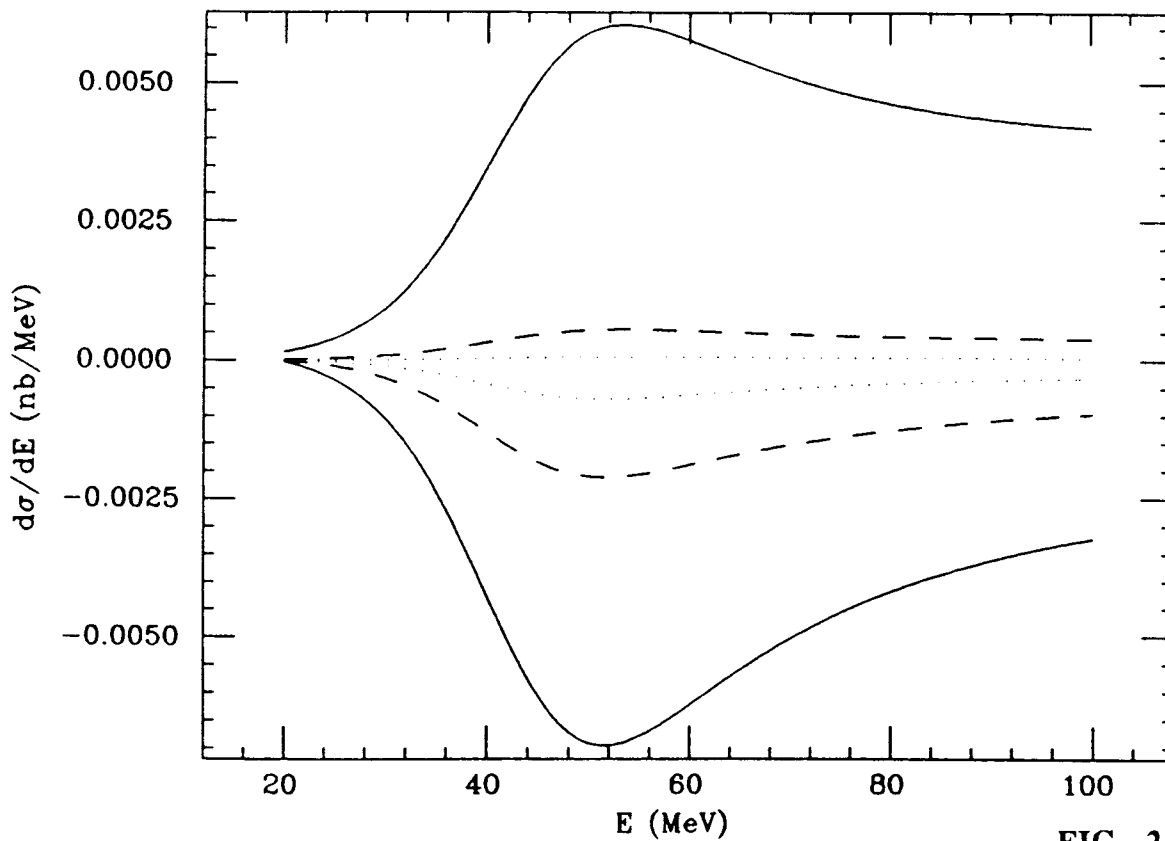


FIG. 2

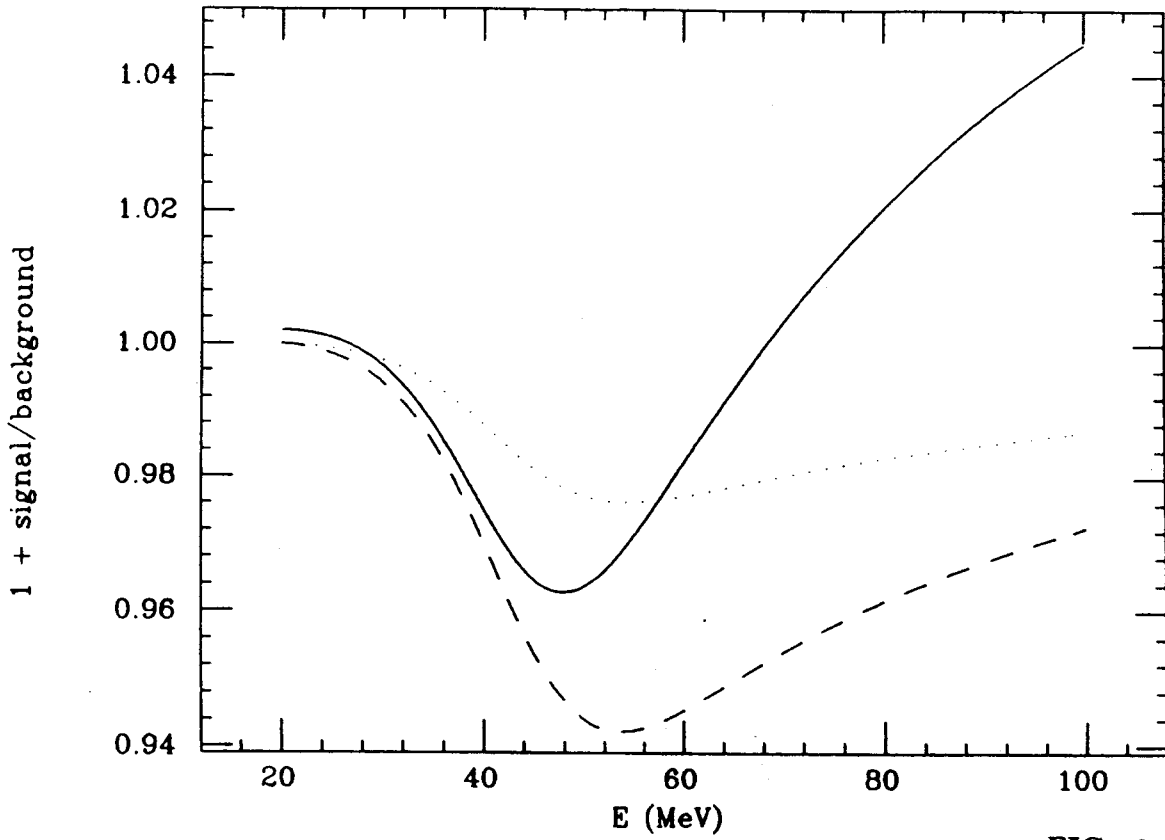


FIG. 3a

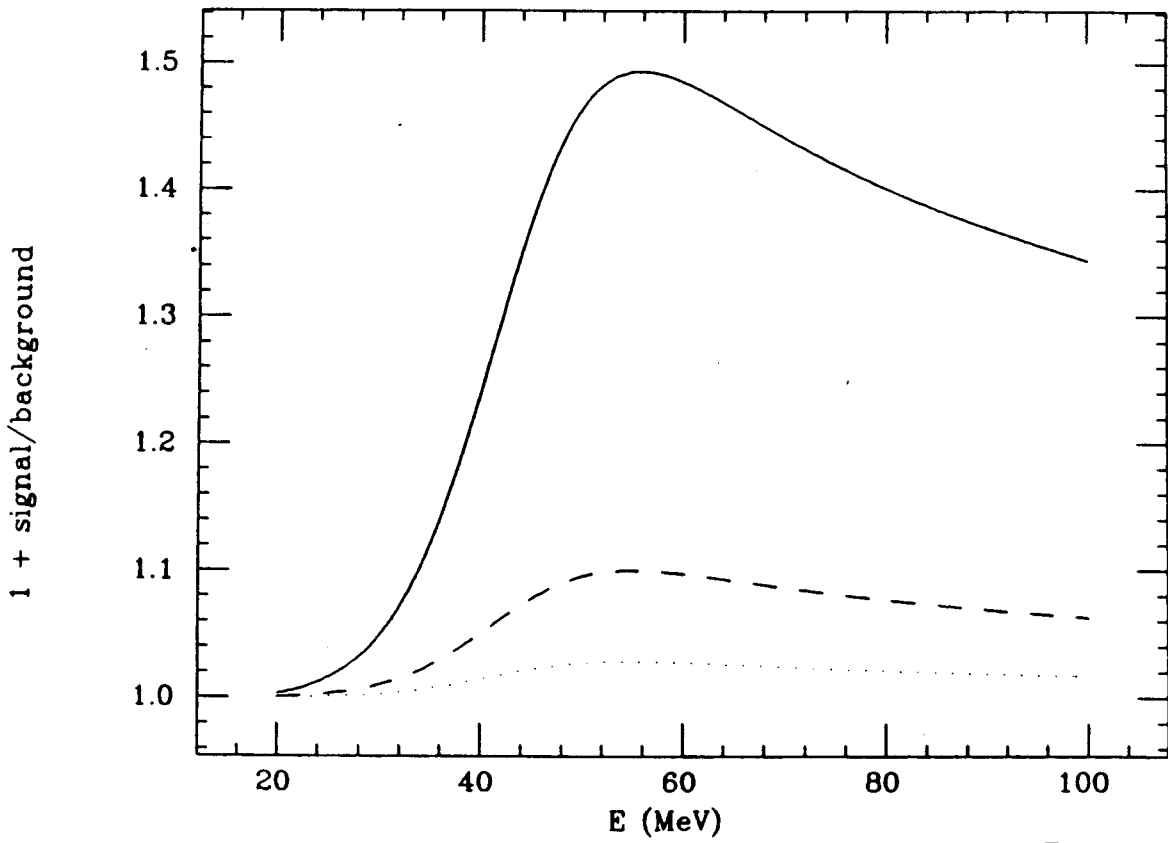


FIG. 3b

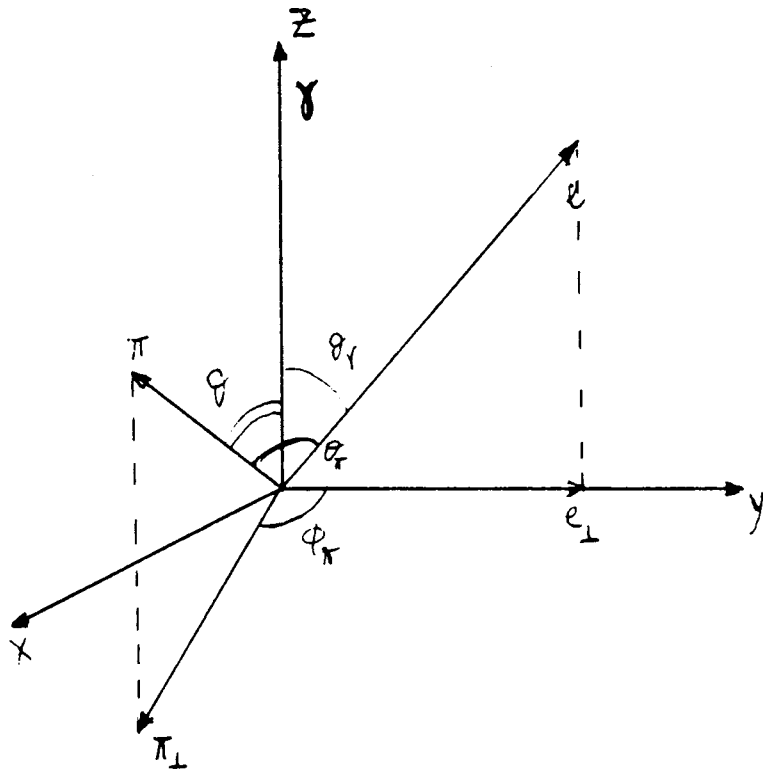


FIG. 4

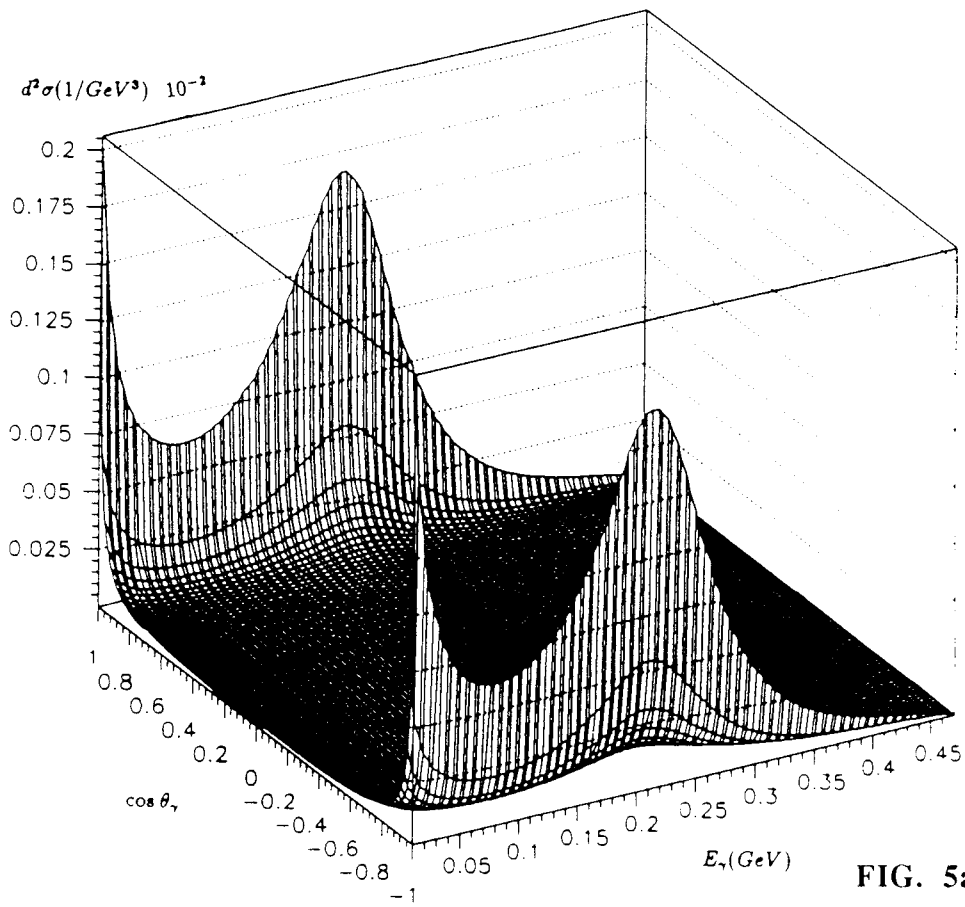


FIG. 5a

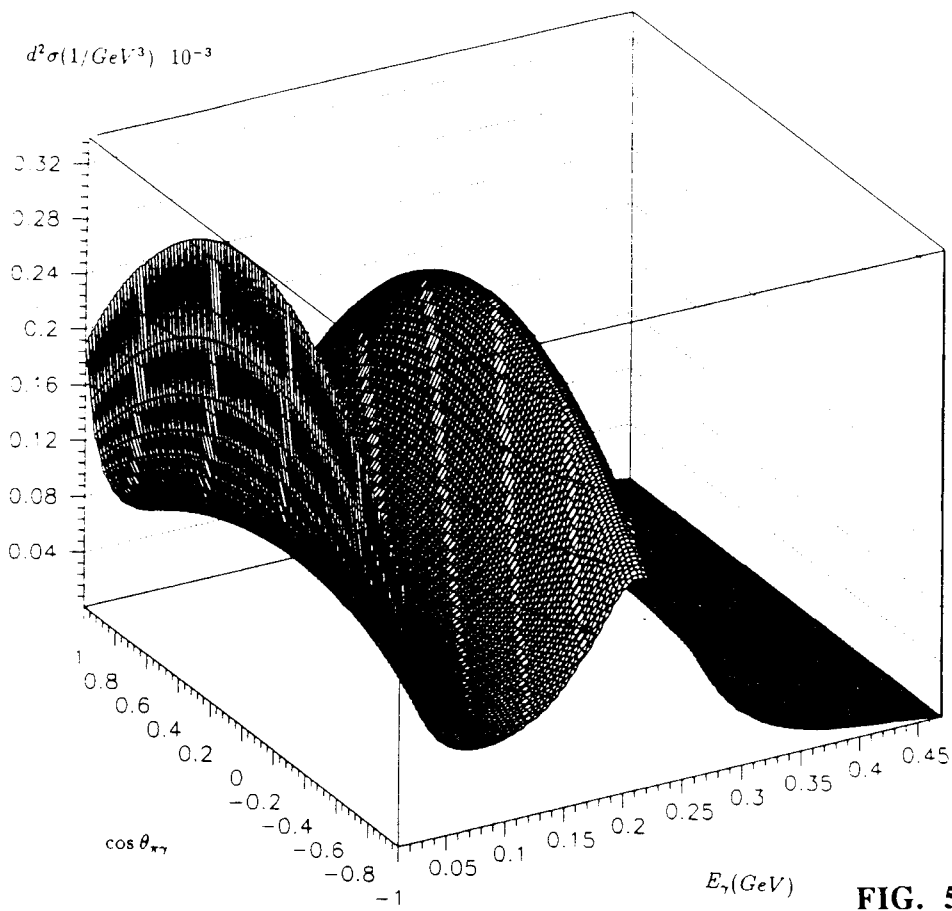


FIG. 5b

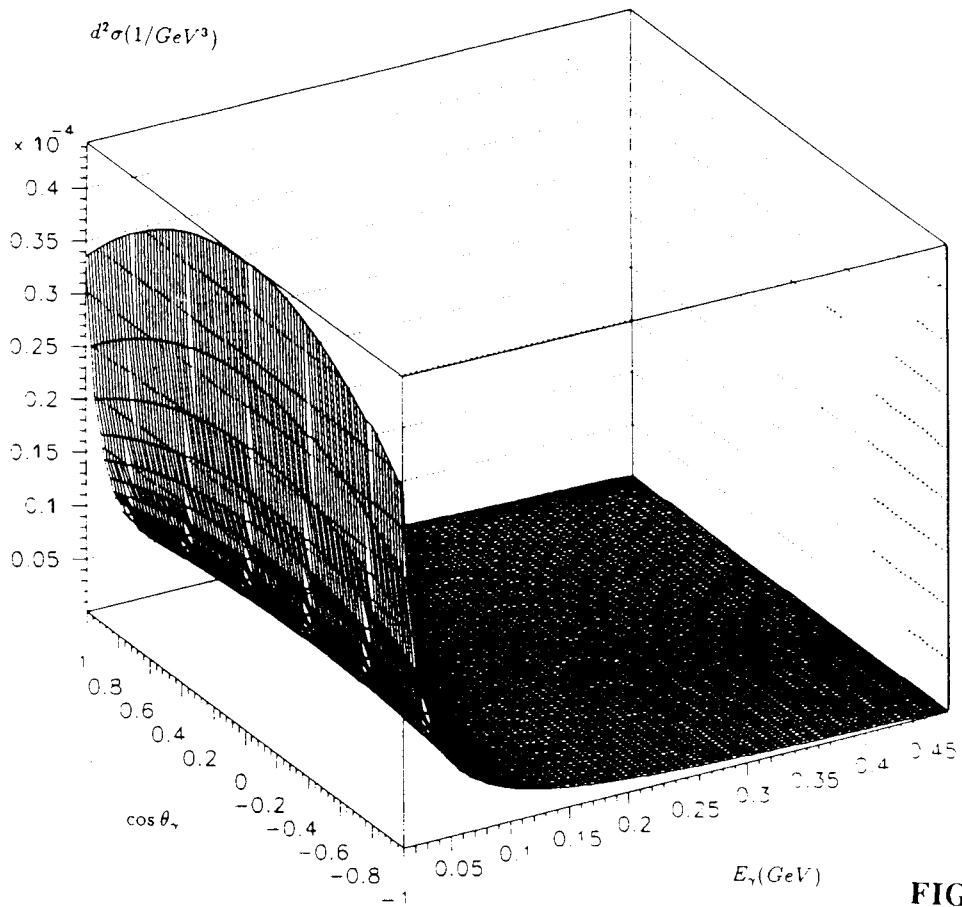


FIG. 6a

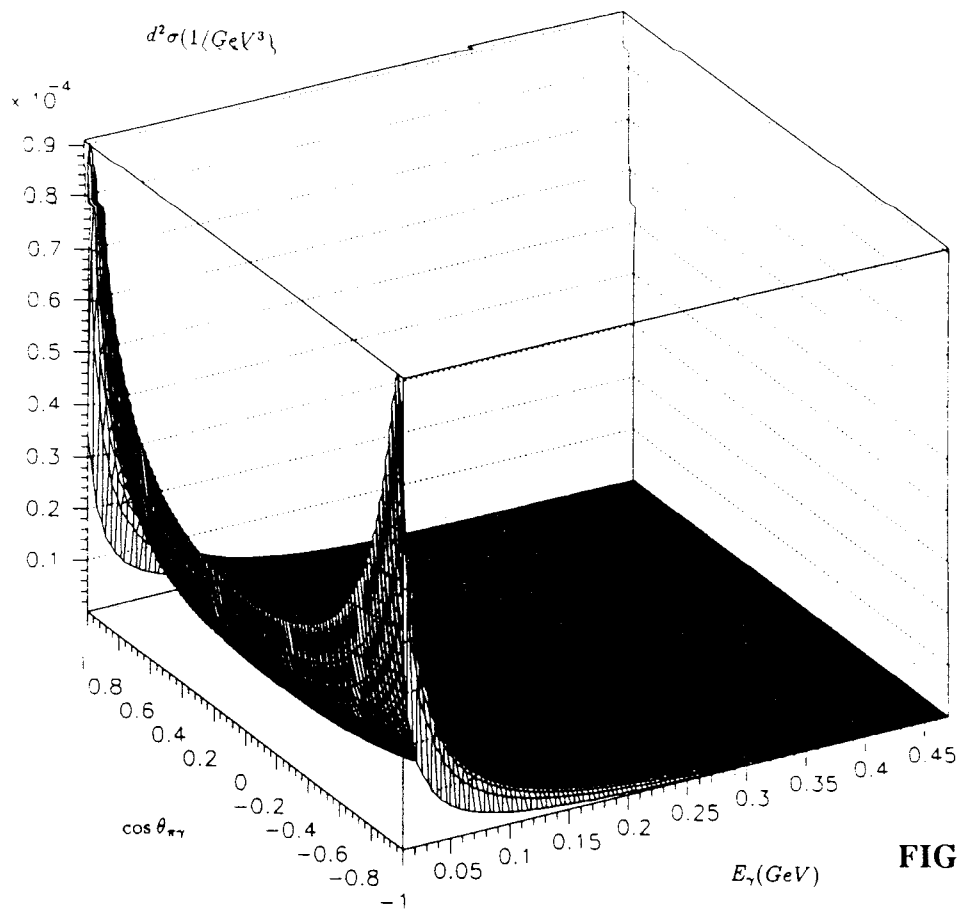


FIG. 6b

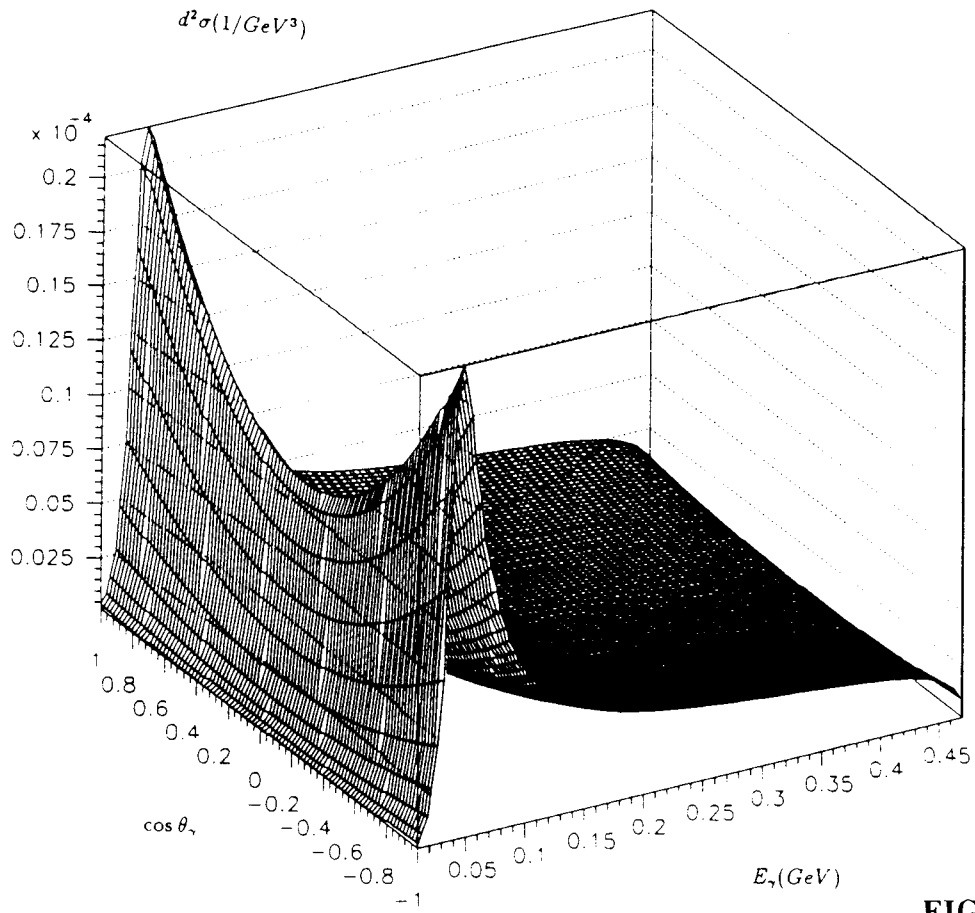


FIG. 7a

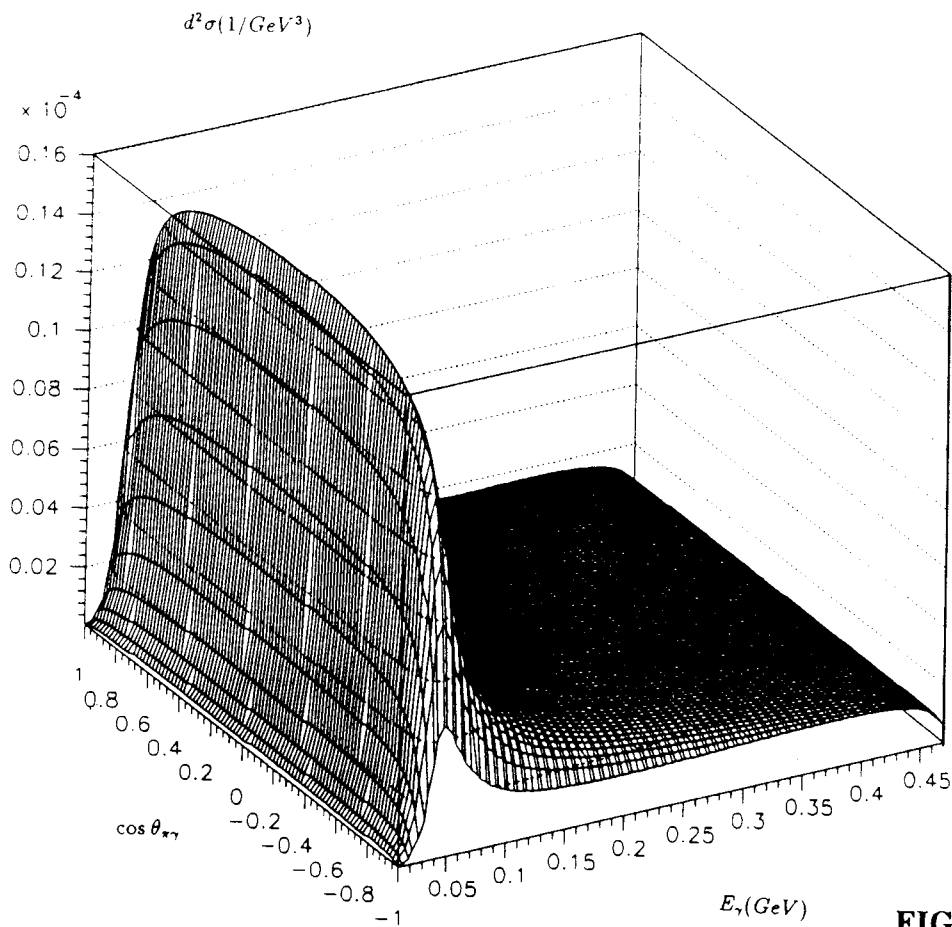


FIG. 7b

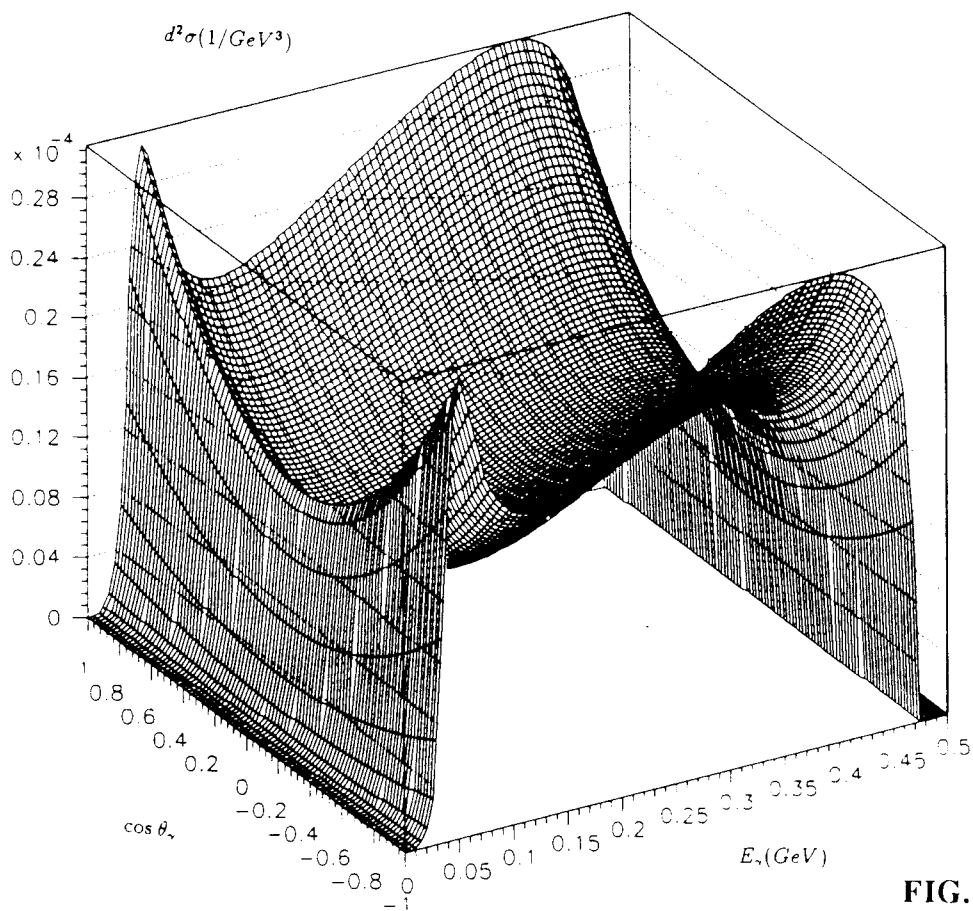


FIG. 8a

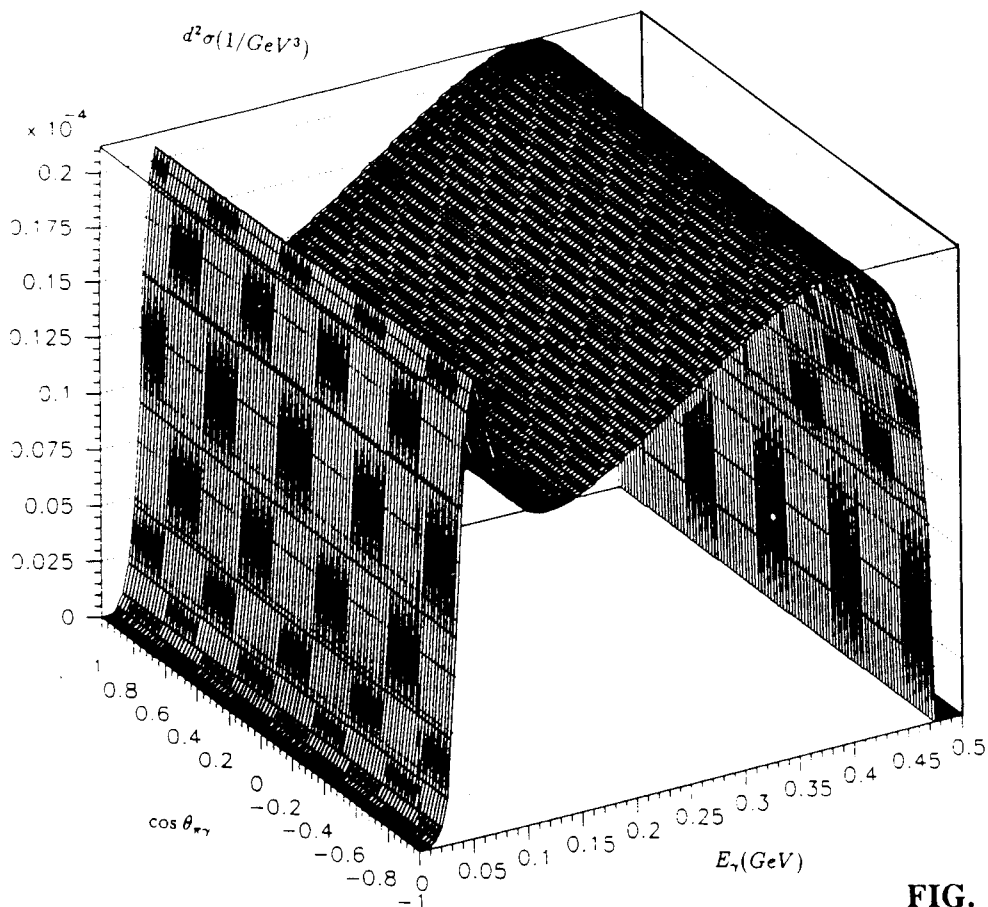


FIG. 8b